Talanta 181 (2018) 24–31

Contents lists available at ScienceDirect

Talanta

journal homepage: www.elsevier.com/locate/talanta

A molecular beacon based on DNA-templated silver nanoclusters for the highly sensitive and selective multiplexed detection of virulence genes

Dan Han, Chunying Wei*

Key Laboratory of Chemical Biology and Molecular Engineering of Ministry of Education, Institute of Molecular Science, Shanxi University, Taiyuan 030006, PR China

ARTICLE INFO

Keywords:
Biosensor
DNA-Ag NCs
HIV
H1N1
H5N1

ABSTRACT

In this work, we develop a fluorescent molecular beacon based on the DNA-templated silver nanoclusters (DNA-Ag NCs). The skillfully designed molecular beacon can be conveniently used for detection of diverse virulence genes as long as the corresponding recognition sequences are embedded. Importantly, the constructed detection system allows simultaneous detection of multiple nucleic acids, which is attributed to non-overlapping emission spectra of the as-synthesized silver nanoclusters. Based on the target-induced fluorescence enhancement, three infectious disease-related genes HIV, H1N1, and H5N1 are detected, and the corresponding detection limits are 3.53, 0.12 and 3.95 nM, respectively. This design allows specific, versatile and simultaneous detection of diverse targets with easy operation and low cost.

1. Introduction

The human immunodeficiency virus (HIV), as a result of destroying and swallowing human T4 lymphocyte, can cause the breakdown of the human immune system and ultimately lead to death, so far there are no effective treatment methods for HIV. Meanwhile, both H1N1 and H5N1 are known as the bird flu viruses, and there is a trend of gradual proliferation because of the propagation of birds and mammals in recent years. Therefore, these viruses should be closely monitored to prevent the epidemics from spreading. Currently, nucleic acid detection is one of the most common detection methods for virulence genes, which is benefit from the high efficiency of the specific recognition between the probe and the target. It is a pity that the conventional nucleic acid probes require usually a pre-labeled signal source including organic molecules and quantum dots, which not only brings the consumption of time and funds but also may suffer from high fluorescence background and even presents the toxicity to organisms [1–4]. And what's more, the existence of an external label most likely has an impact on the interactions of probes with targets [3]. Even if some nucleic acid probes such as intercalating organic dyes avoid the pre-label, they still suffer from the false positive response because of the non-specific interactions with biomolecules and are also sensitive to photobleaching. All of these limit their applications in practical detection [3,4]. Therefore, the development of easy of design and synthesis, inexpensive, environment-friendly nucleic acid probe is urgently needed to make up for these deficiencies.

In recent years, the silver nanoclusters (Ag NCs) as a novel fluorophore have attracted the increasing attention in the fields of biosensing and bioimaging. In particular, the Ag NCs synthesized using DNA as the template (DNA-Ag NCs) possess the advantages of facile synthesis, tunable fluorescence emission (ranging from visible to near-IR), high fluorescence quantum yields, low toxicity, good photostability, and biocompatibility, so they are extensively applied in the detections of metal ions [5–7], small biomolecules such as ATP, adenosine, biological thiols, and theophylline [8–10], and protein [8,11–14], DNA [3,15–20], and microRNA [20,21]. Furthermore, Many theoretical studies suggest that the cytosine (C) has the stronger binding affinity to Ag^+ than the other bases (G, A, T, U). For this reason, the C-rich single-strand DNA (ssDNA) is most commonly used to synthesize DNA-Ag NCs [22–25].

Herein, based on the specific recognition ability between DNA bases and unique fluorescent properties of DNA-Ag NCs, a fluorescent sensor system for virulence genes was constructed. The fundamental principle of sensor is on account of the release of the C-rich ssDNA sequence induced by the target gene, and the released C-rich ssDNA sequence is an excellent template for the growth of Ag NCs. The strong fluorescence signal of the as-synthesized DNA-Ag NCs succeeds in realizing the qualitative and quantitative detection of the multi-target genes.

2. Experimental section

2.1. Materials and methods

All DNA sequences used in our work were synthesized by Shanghai Sangon Biotechnology Co (Shanghai, China) and were showed in Table

* Corresponding author.
E-mail address: weichuny@sxu.edu.cn (C. Wei).

https://doi.org/10.1016/j.talanta.2017.12.049
Received 5 September 2017; Received in revised form 30 November 2017; Accepted 14 December 2017
Available online 19 December 2017
0039-9140/ © 2017 Elsevier B.V. All rights reserved.

S1. Silver nitrate ($AgNO_3$, 99.8%), sodium borohydride ($NaBH_4$, 98%), and magnesium nitrate [Mg $(NO_3)_2{\cdot}6H_2O$, 99.0%] were supplied by Aladdin Bio-chem technology Co. Ltd. (Shanghai, China). Agarose [Gel Strength (1%) 750 gr /cm^2, gelling temperature: 37 ± 1.5 °C] was purchased from Beijing TransGen Biotech Co., Ltd. Phosphate buffer solution (PBS) (20 mM, pH 7.0) was used in the whole experimental process. All solutions were prepared or diluted with Milli-Q water.

UV–vis absorption measurements were carried out with a Cary 50 Bio spectrophotometer (Varian Inc., CA). Fluorescence spectra were obtained at room temperature by a Cary Eclipse Fluorescence Spectrophotometer (Varian Inc. CA) and a Fluoromax-4 Spectrofluorometer (Horiba Jobin Yvon Inc., France). Both excitation and emission spectra were recorded with 5 nm slit widths. CD Spectra were recorded by a Chirascan Circular Dichroism spectrophotometer (Applied Photophysics Ltd., Surrey, UK) at room temperature. The spectra were scanned in the wavelength range of 220–320 nm at the scanning speed of 120 nm/min and 1 nm bandwidth. The concentration of DNA-Ag NCs was 2.5 μM and the scan of the buffer alone was subtracted from the average scan for each sample. The final measurements were represented by the average of three scans. The particle sizes of the synthesized DNA-Ag NCs were characterized with transmission electron microscopy (TEM) using a JEOL JEM-2100 high resolution TEM instrument operated at 200 kV. Gel electrophoresis analysis was carried out with a DYY-6C electrophoresis apparatus (Liuyi Instrument Factory, Beijing, China), and the gel was scanned using the Alpha Imager (USA). The luminescence decay curves were measured on FL920 fluorescence lifetime spectrometer (Edinburgh Instruments, Livingston, UK) operating in the time-correlated single photon counting (TCSPC) mode equipped with 405 nm pulsed laser as the excitation source. As for data analysis, the commercial software provided by Edinburgh Instruments was run. The picosecond transient fluorescence decays were fitted with multi-exponential (*n*) function and the average excited state lifetime was expressed by the equation: $\tau_{avg} = \sum_{i=1}^{n} A_i \tau_i$, when $\sum_{i=1}^{n} A_i = 1$.

2.2. Preparation of DNA-Ag NCs

First, the corresponding DNA solution of 2.5 μM was prepared in advance in 20 mM PBS at pH 7.0 (with 5.0 mM Mg^{2+} for the HIV and H5N1 detection systems and Mg^{2+}-free for the H1N1 detection system). Then the $AgNO_3$ solution of 15 μM was added into the prepared corresponding DNA solution. Next, after incubating at 4 °C for 15 min, the freshly prepared $NaBH_4$ solution was added to the above mixture and shaken vigorously for 1 min (molar ratio of Ag^+: $NaBH_4$: DNA = 6: 6: 1). Finally, the mixed solution was further stored in the dark at 4 °C for 2–3 h to prepare DNA-Ag NCs. Unless otherwise noted, the concentrations of all solutions used in the experiments were consistent with that of the corresponding solution mentioned above.

2.3. Agarose gel electrophoresis

Three groups of DNA samples (HIV probe 4, HIV probes 4/HIV, HIV probes 4/HIV/Ag NCs; H1N1 probe, H1N1 probe/H1N1, H1N1 probe/H1N1/Ag NCs, and H5N1 probe, H5N1 probe/ H5N1, H5N1 probe/H5N1/Ag NCs) were prepared in 20 mM PBS (pH 7.0), and 8 μL of each DNA samples were thoroughly mixed with 2 μL of loading buffer. Then, 8 μL of the mixed samples were added into the sample holes of the prepared gel. The 1.5% agarose gels electrophoresis analysis of DNA samples was operated in the TAE buffer (pH 7.0) at a constant voltage of 100 V for 45 min at room temperature. Finally, the gel was scanned using the Alpha Imager (USA).

2.4. Sensing of target DNA

In the process of the sensing detection, 2.5 μM hairpin probe solution was firstly prepared by annealing. Then, different concentrations of target genes (HIV, HIN1, or H5N1) were individually added into the probe solution. The mixed DNA solutions were incubated for 2 h at room temperature with gentle shaking, and then the DNA-Ag NCs were synthesized according to the above procedures. After that the fluorescence or other measurements were performed immediately. In addition, a single-base mismatched DNA was added in place of target DNA with the same experimental process to evaluate the selectivity of the probe.

2.5. Multiplexed fluorescent sensing of target DNA

In the multiplexed fluorescent detection of targets, five groups of experiments were carried out. Firstly, 2.5 mL of 7.5 μM probe solution (HIV, H1N1, or H5N1) was annealed in the respective buffer with or without 5.0 mM Mg^{2+} by heating at 85 °C for 15 min and gradually cooling to the room temperature. Next, the three annealed probe solutions were mixed and divided equally into the parallel five groups. Next, 2.5 μM targets H1N1, H5N1, and HIV and their mixtures were added respectively to the above four sets of parallel probe mixtures and further incubated for 2 h to form duplex. The remaining one group only containing annealed probe mixture was considered as a control experiment. Finally, $AgNO_3$ (45 μM) was added into the aforementioned five mixtures and kept at 4 °C for 15 min, and then the freshly prepared $NaBH_4$ (45 μM) was also introduced and shaken vigorously for 1 min. After that, the five mixtures were stored in the dark at 4 °C for 2–3 h to prepare DNA-Ag NCs.

2.6. Detection of target DNAs in fetal bovine serum

The fetal bovine serum was diluted 100 times with reaction buffer in the first place. Then the target DNA was detected in the 1% fetal bovine serum samples in accordance with the procedures in PBS buffer.

3. Results and discussion

As shown in Fig. 1, the working principle of the sensor system is based on target-triggered fluorescence enhancement on account of generation of fluorescent DNA-Ag NCs. The designed molecular beacon is mainly composed of three domains: the sequence for the formation of Ag NCs (blue part, C-rich sequence), the recognition sequence of target DNA (black part, loop region), and the blocking sequence (purple part). As a result of the Watson-Crick complementary between the blocking segment and the segment responsible for the formation of Ag NCs, the probe annealed in PBS buffer can self-assembled into a stable hairpin structure (Fig. S1 ESI†), and the formation of DNA-Ag NCs is prohibited. However, once the target DNA is introduced, the hairpin structure of probe unfolds and forms a stable duplex structure with target due to the stronger hybridization between the target DNA and its complementary sequence (loop region in the probe). Thus the C-rich DNA segment is liberated from the blocking sequence and then DNA-Ag NCs are synthesized in the presence of $AgNO_3$ and $NaBH_4$. It is the fluorescence of DNA-Ag NCs that provides a readout signal for sensing detection. Fortunately, the molecular beacon can be used for specific and versatile detection of diverse targets by just replacing the recognition sequence. And what's more, if we can circumvent overlap of emission spectra, the proposed molecular beacon will be also used to detect simultaneously the multiple nucleic acids. In this work, we fulfills the simultaneous detection for the human immunodeficiency virus (HIV) gene, avian influenza virus H1N1 and H5N1 genes based on the aforementioned sensing platform. Furthermore, the sensor system can also detect the three genes in serum sample.

3.1. Characterization of DNA-Ag NCs

In principle, when certain concentration target is introduced to the hairpin probe solution, the sensor should show an obvious fluorescence enhancement. However, the properties of DNA-Ag NCs are highly dependent on the sequence, length and secondary structure of DNA template [26–29], which is the reason why we select four different C-

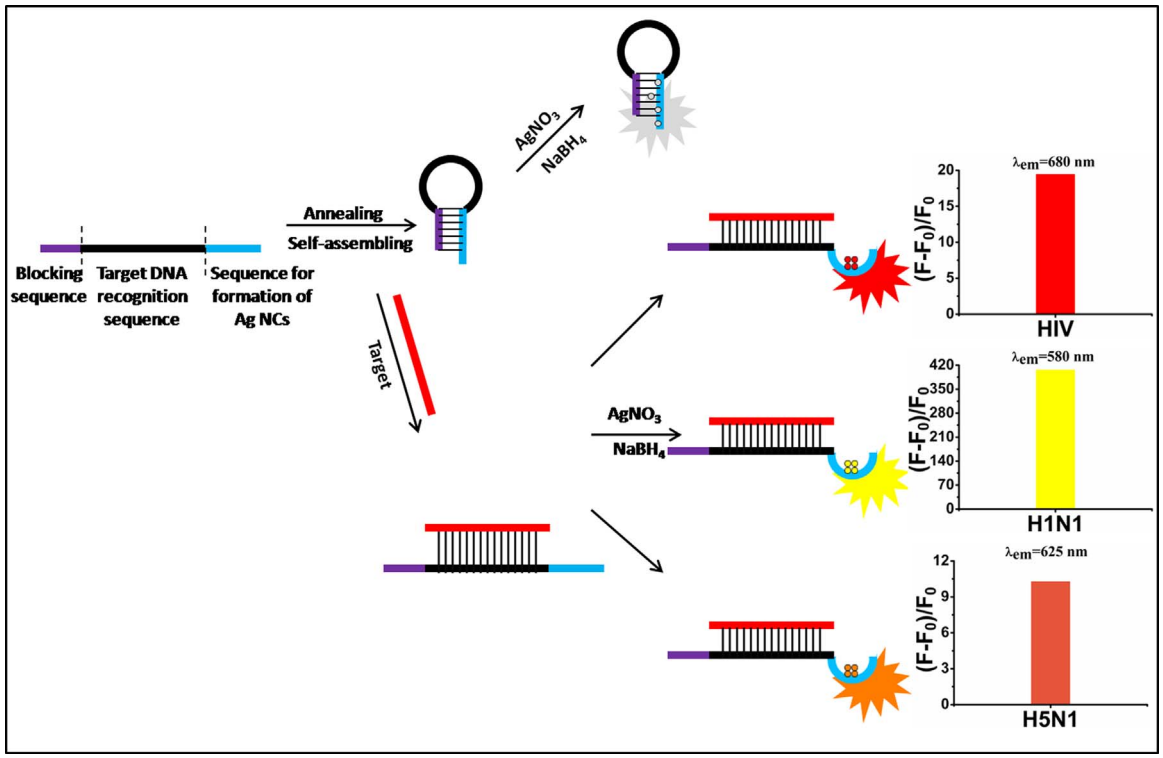

Fig. 1. Schematic illustration of the detection of the target DNA based on the fluorescence enhancement induced by hybridization of the target and the hairpin DNA probe.

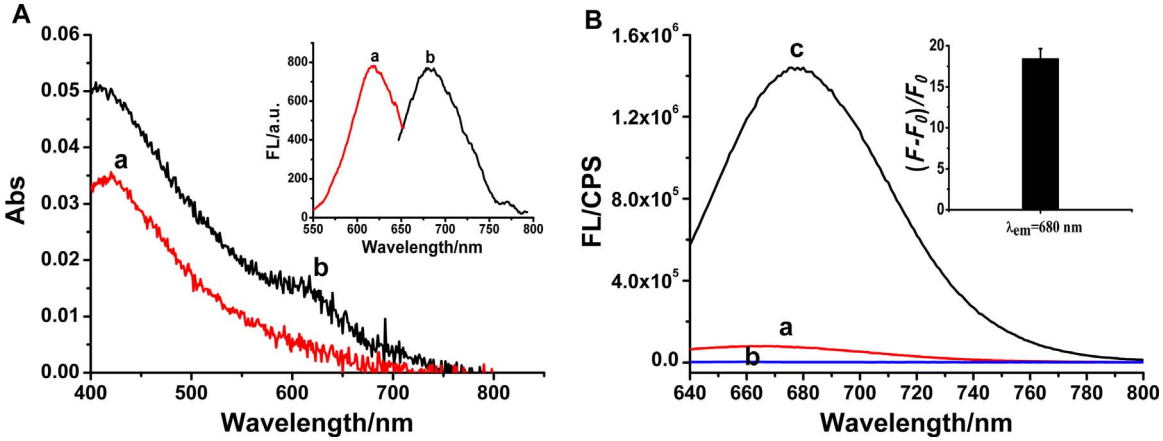

Fig. 2. (A) UV–vis absorption spectra of the silver species synthesized with HIV probe 4 (curve a) and HIV probe 4 + HIV (curve b). The inset is fluorescence excitation (curve a) and emission (curve b) spectra of Ag NCs synthesized with HIV probe 4 + HIV. (B) Fluorescence emission spectra of DNA-Ag NCs under the different conditions: (a) HIV probe 4; (b) HIV; (c) HIV probe 4 + HIV. The inset is that the relative fluorescence intensity $(F\text{-}F_0)/F_0$ recorded in the response of HIV gene to HIV probe 4. F and F_0 represent the emission intensity of synthesized Ag NCs in the presence and absence of HIV, respectively. Error bars are calculated from three parallel experiments.

rich ssDNAs as templates to design four probes (HIV probes 1, 2, 3, and 4 in Table S1 ESI†) for HIV gene detection. Excitingly, the fluorescent enhancement of the probe 4 shows a significant superiority over that of HIV probes 1, 2, and 3 upon associating with the target HIV (Fig. S2 ESI†). In the process of annealing, the HIV probe 4 self-assembles into the hairpin structure (Fig. S1A ESI†) so that the C-rich DNA sequence for synthesis of Ag NCs is locked. Because of the lack of the template for stabilizing Ag NCs, the silver atoms aggregate to form the large Ag nanoparticles instead of ultrasmall Ag NCs. So the only strong peak at ~420 nm (curve a, Fig. 2A) originates from the plasmon resonance absorption of the larger Ag nanoparticles that have no sequence specificity. On the contrary, once the target HIV is added to the probe solution, the hairpin probe is unlocked and releases the C-rich DNA sequence. Ultimately, the DNA-Ag NCs are synthesized and emit the fluorescent signal. Therefore, the other new absorption peak around 620 nm is also observed apart from the absorption peak generated by Ag nanoparticles (Fig. 2A, curve b), which is assigned to the characteristic peak of DNA-Ag NCs [23,30–33]. DNA-Ag NCs show a maximum emission at 680 nm (Fig. 2A inset, curve b) when excited at 620 nm (curve a). To further assess the feasibility of our sensing mechanism, the fluorescence emission spectra are recorded under the different circumstances. As we expected, the system exhibits very weak fluorescence emission when the probe (Fig. 2B, curve a) or the target (curve b) exists alone, which excluded the possible contribution of the probe and the target themselves to the synthesis of Ag NCs. When the target HIV is added, the fluorescence intensity of system increases almost 20-fold (curve a, c and inset in Fig. 2B). These results indicate that the target DNA can open the hairpin probe and release C-rich sequence that is used as the template to synthesize the fluorescence DNA-Ag NCs.

Inspired by the design of the HIV probe 4, the other two detection

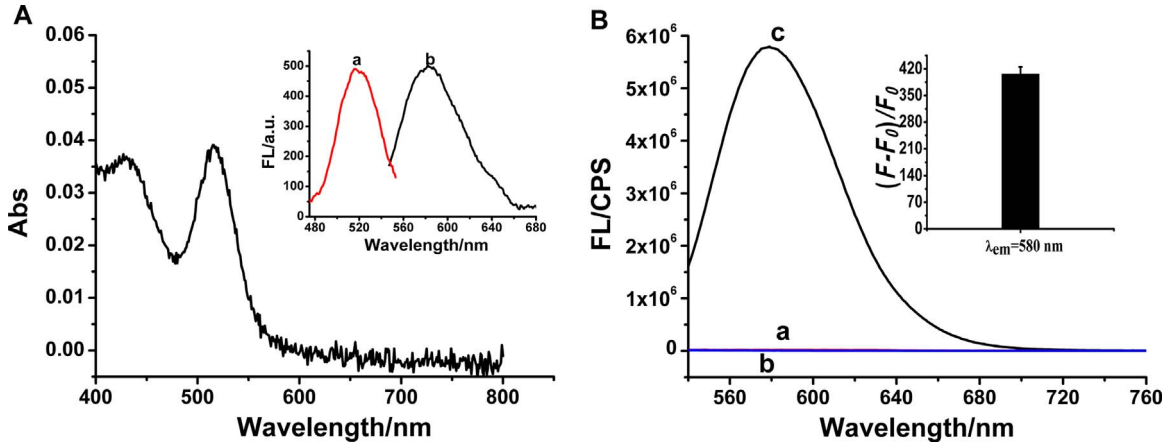

Fig. 3. (A) UV–vis absorption spectra of the silver species synthesized with the H1N1 probe + H1N1 in PBS buffer. The inset is fluorescence excitation (curve a) and emission (curve b) spectra of silver species synthesized in the H1N1 probe + H1N1 solution. (B) Fluorescence emission spectra of DNA-Ag NCs in different situations: (a) the hairpin H1N1 probe; (b) H1N1; (c) the H1N1 probe + H1N1. The inset is that the relative fluorescence intensity $(F\text{-}F_0)/F_0$ recorded in the response of H1N1 gene to H1N1 probe. F and F_0 represent the emission intensity of Ag NCs in the presence and absence of HIV, respectively. Error bars are calculated from three parallel experiments.

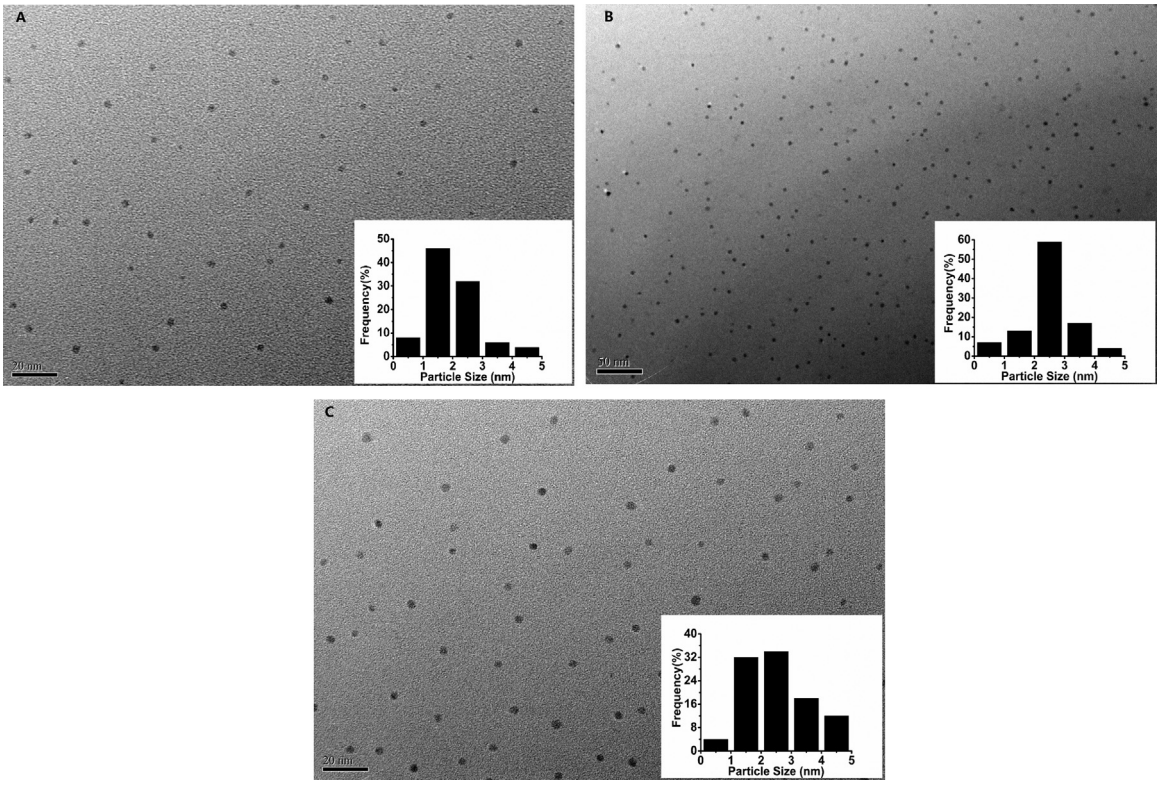

Fig. 4. TEM images of DNA-Ag NCs synthesized by HIV probe 4/HIV(A), H1N1 probe/H1N1(B), and H5N1 probe/H5N1(C). The inset shows the size distribution histogram.

probes are also constructed and give the positive responses for the corresponding target genes H1N1 and H5N1 (Table S1 ESI†). Interestingly, the fluorescence properties of DNA-Ag NCs synthesized in three different sensor systems are distinct. Among them the H1N1 probe presents the best biosensor result. Comparing with H1N1 probe alone, the fluorescence intensity of the system containing both the probe and target increases dramatically by 400 times when excited at 520 nm (Fig. 3). While the fluorescence intensity increases only about 10-fold for the system containing the H5N1 probe and H5N1 gene compared with the H5N1 probe alone (Fig. S3 ESI†). Furthermore, we clearly observe that the maximum emission wavelengths shift to the long wavelengths with the increasing excitation wavelengths for both H5N1 and HIV detection systems (Fig. S4A and S4C ESI†). However, the maximum emission wavelength of the H1N1 detection system remains at 580 nm when the excitation wavelengths is changed from 480 to 540 nm (Fig. S4B ESI†). Their fluorescence intensities are also dependent on the excitation wavelengths, which is similar to the observed phenomenon for most organic dyes. In addition, their maximum emission wavelengths of synthesized Ag NCs are different obviously and the values are 580, 625, and 680 nm for H1N1, H5N1, and HIV biosensors, respectively, and the large difference in the maximum emission wavelength can be used to detect these targets simultaneously (see below). Based on the analysis for the three DNA-Ag NCs, it is concluded that the sequence, length, and secondary structure of the adjacent bases of the template DNA can regulate fluorescence properties of the DNA-Ag NCs by influencing the structural heterogeneity of as-synthesized clusters, including size, composition, and structure [24,25,34,35]. Of course, the in-depth investigations on the properties of these DNA-Ag NCs by other

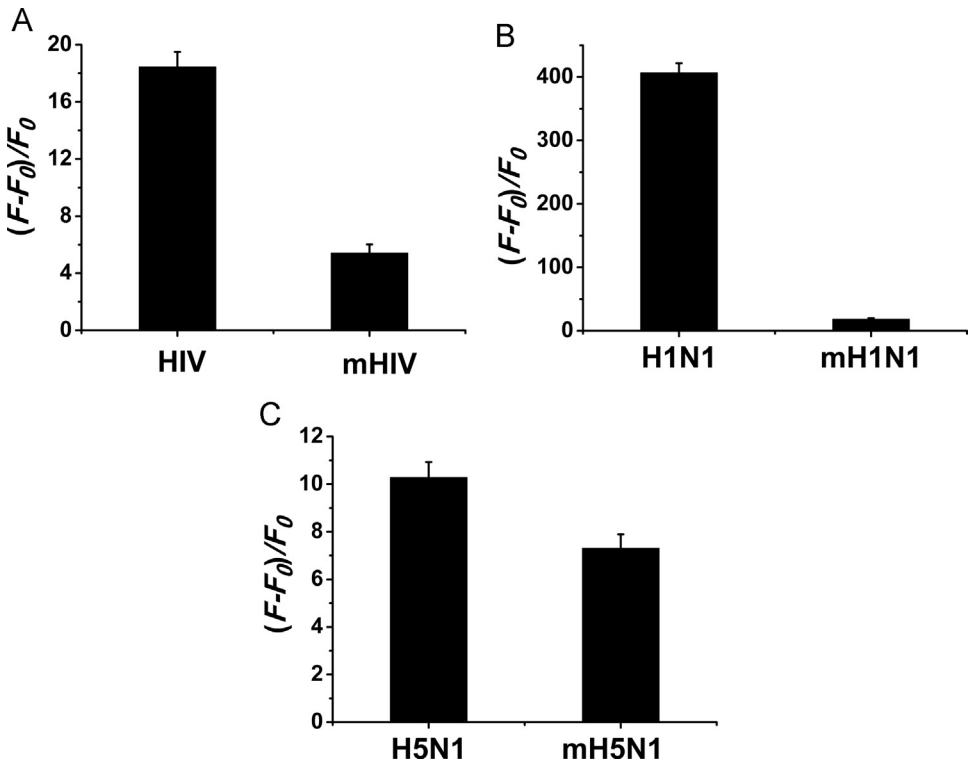

Fig. 5. The specificity detection of the assay for HIV (A), H1N1(B), and H5N1(C). The relative fluorescence intensity is recorded as $(F\text{-}F_0)/F_0$, where F and F_0 represent the emission intensity of Ag NCs in the presence and in the absence of target DNA or *m*DNA, respectively. Error bars are calculated from three parallel experiments.

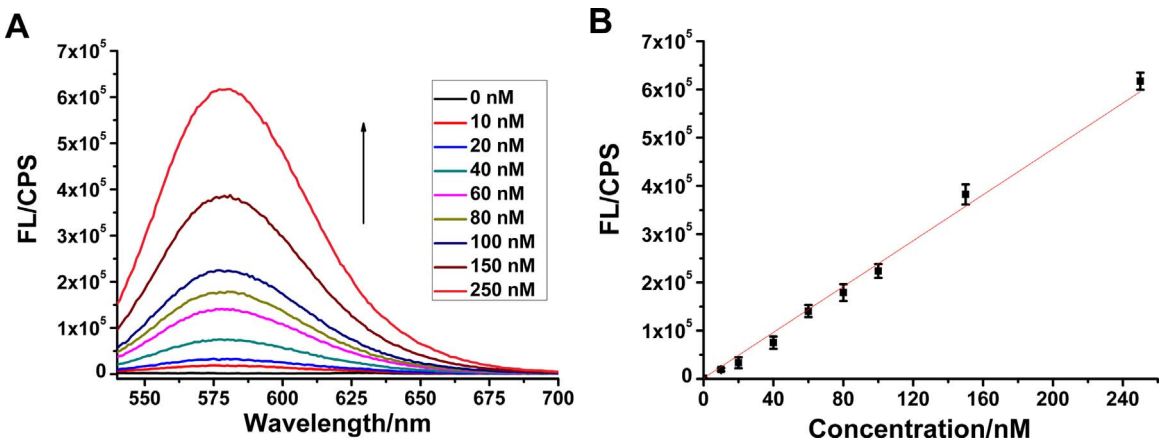

Fig. 6. (A) The fluorescence emission of DNA-Ag NCs when the varying concentrations (from 0 to 250 nM) of H1N1 gene are added. (B) The linear relationship between the fluorescence intensity and the concentration of H1N1 gene ranging from 0 to 250 nM.

methods are necessary.

The incubation time with $NaBH_4$ is crucial to the synthesis of the fluorescence DNA-Ag NCs, and different DNA strands usually require different incubating time so as to form fluorescence DNA-Ag NCs. Here, we optimize respectively the incubation time of different targets with $NaBH_4$ to improve the sensing performance of the fluorescence light-up system. The $(F\text{-}F_0)/F_0$ value is employed to evaluate the effect of incubation time on the properties of DNA-Ag NCs. Based on these results shown in Fig. S5 (ESI†), the optimized incubation times for the sensing systems of the HIV, H1N1, and H5N1 are 3, 2, and 2 h, respectively, and the optimal time are used throughout in the experiments.

The conformational changes of the DNA probe, the probe-target, and the probe-target-Ag NCs are further demonstrated by gel electrophoresis analysis, as indicated in Fig. S6. The systems consisting of the probe and the target, HIV probe 4/HIV (lane 2), H1N1 probe/H1N1 (lane 5) and H5N1 probe/H5N1 (lane 8), present the bands with significantly slower migration rate relative to HIV probe (lane 1), H1N1 probe (lane 4), and H5N1 probe (lane 7) alone, which indicates that the probe and the target form the stable duplex structure. In addition, When Ag NCs are synthesized on the as-formed duplex, the shifts of the bands of HIV probe 4/HIV-AgNCs (lane 3), H1N1 probe/H1N1-AgNCs (lane 6), and H5N1 probe/H5N1-Ag NCs (lane 9) are consistent with those of their corresponding duplexes without Ag NCs, and no obvious ssDNA band is observed, suggesting that the as-synthesized Ag NCs on the DNA templates have no effect on the stability of the already formed DNA duplex. CD spectroscopy is a valuable technique used for characterizing the conformation of nucleic acids [36,37], as an example, CD spectra of the H1N1 probe/H1N1 and H1N1 probe/H1N1 target-Ag NCs are measured to further confirm their secondary structures (Fig. S7 ESI†). It is found that the as-synthesized DNA-Ag NCs present a strong positive peak at 280 nm and a negative peak at 250 nm, which is the characteristic of duplex DNA, indicating the maintenance of the duplex structure [37].

Transmission electron microscopy (TEM) is also utilized to characterize the DNA-Ag NCs. As shown in Fig. 4, the DNA-Ag NCs are well dispersed when the target is added and the average diameters are all

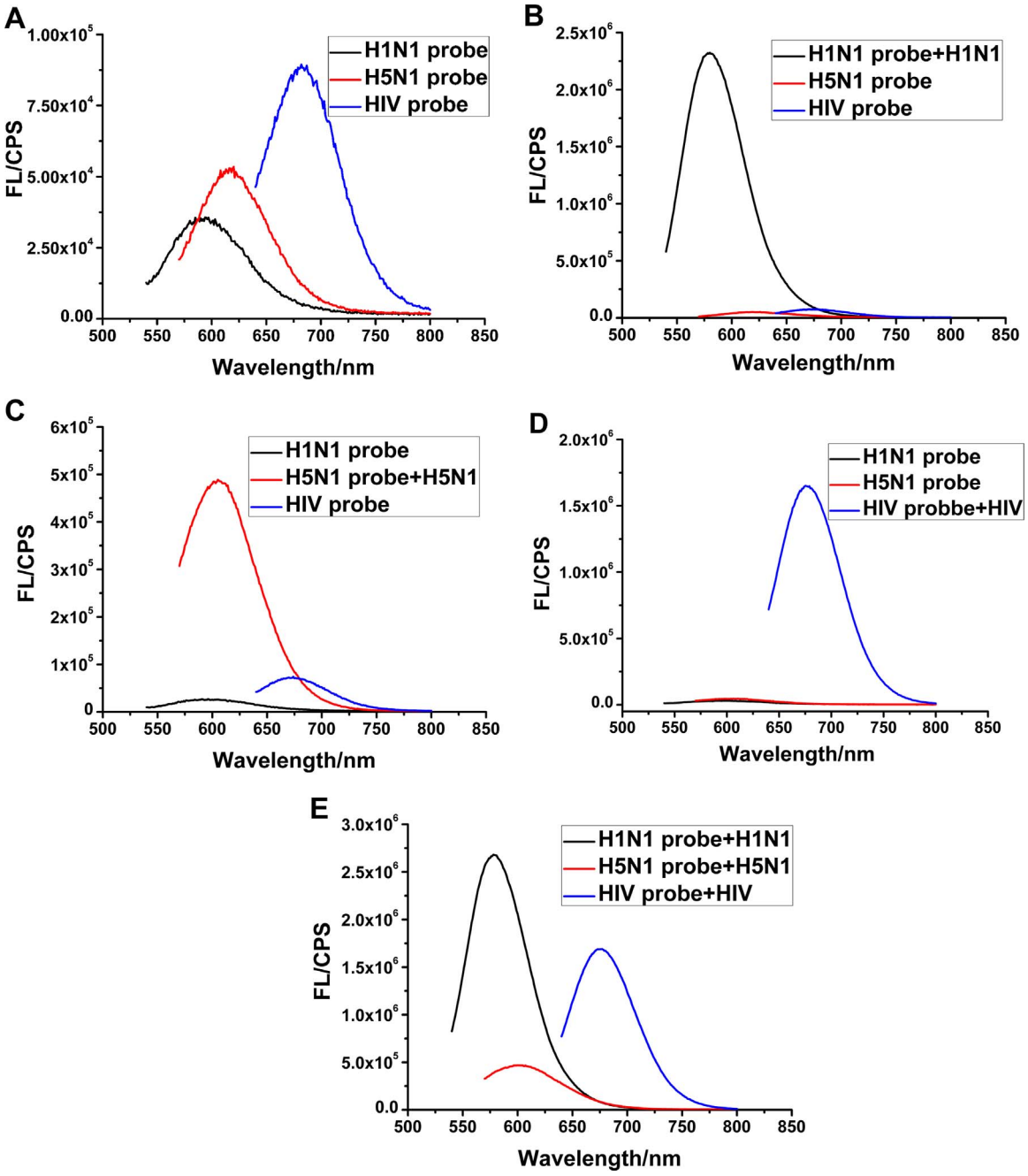

Fig. 7. Fluorescence emission spectra of multiplexed detection for H1N1, H5N1, and HIV. (A) In the absence of target DNA; (B) In the presence of 2.5 μM H1N1, H5N1, and HIV targets; (C) In the presence of 2.5 μM H1N1 target only; (D) In the presence of 2.5 μM H5N1 target only; (E) In the presence of 2.5 μM HIV target only. Excitation and emission wavelengths are 520 nm and 580 nm for the H1N1 probe /H1N1-AgNCs, 550 nm and 605 nm for the H5N1 probe /H5N1-AgNCs, and 620 nm and 680 nm for the HIV probe 4/HIV-AgNCs, respectively.

around 2–3 nm for the three kinds of DNA-Ag NCs. Moreover, we can observe intuitively and clearly that the Ag NCs synthesized by the H1N1 probe/target present more uniform size and distribution and the size of particle is mainly ~2.5 nm. While the other two DNA-Ag NCs give a much broader size distribution, which further explains the reason that the fluorescence properties of the H1N1 probe/H1N1-Ag NCs are more excellent than those of the HIV probe 4/target- and the H5N1 probe/target-Ag NCs. Furthermore, we measure the lifetimes of DNA-Ag NCs synthesized by the probe or the probe/target with the time-correlated single photon counting (TCSPC) technique and the decay curves are fitted with a biexponential or triexponential decay convoluted by the instrument response function (Figs. S8-S10 ESI†). The values of the lifetime are listed in Table S2 (ESI†). For the HIV gene, the average lifetime of dark DNA-Ag NCs is 2.80 ns while the average lifetime of bright DNA-Ag NCs is 3.46 ns. In the case of the H1N1 gene the average lifetimes of dark DNA-Ag NCs and bright DNA-Ag NCs are 1.27 and 1.42 ns, respectively. Similarly, the average lifetimes of the DNA-Ag NCs of the H5N1 probe alone or with the target are 2.47 ns and 2.51 ns, respectively. Based on the obtained results, no obvious changes are observed for the fluorescence lifetimes of both the probe-Ag NCs and the probe/target-Ag NCs.

3.2. Selectivity and sensitivity

High selectivity is one of the essential elements of an excellent biosensor. To evaluate the specificity of the sensing system, we investigate the response of the probe towards the single-base mismatched sequence (*m*DNA, Table S1 ESI†). From the results given in Fig. 5, the

fluorescence intensity of the *m*DNA/probe-Ag NCs decreases significantly compared to that of the target DNA/probe-Ag NCs under the same conditions. These results indicate that the Ag NCs-based molecular beacon has excellent selectivity for the target and is able to distinguish the single-base mismatched sequence.

The fluorescent response of the target DNA at different concentrations is investigated to examine the analytical performance of the sensing system. As shown in Fig. 6 and Fig. S11 and S12 (ESI†), the fluorescence intensities of three systems increase gradually with the increasing concentrations of the target DNA. At the same time, a good linearity relationship are found in the range from 5 to 2000 nM (R^2 = 0.990) for HIV, 0–250 nM (R^2 = 0.993) for H1N1, and 50–500 nM (R^2 = 0.988) for H5N1, and their corresponding detection limits ($3\sigma/K$, where σ is the standard deviation of the blank solution and K is the slope of the calibration curve) are 3.53, 0.12, and 3.95 nM, respectively, which are comparable to and even superior to some previously reported results from the fluorescence methods (Table S3).

3.3. Multiplexed fluorescence detection of target DNA

It is generally known that simultaneous sensing of multiple targets is still a challenge in the bioanalysis field. Here, we are delighted to find that the proposed molecular beacon in this work allows simultaneous detection of different targets. As shown in Fig. 7, only very weak fluorescence emission is detected for the mixture of three probes (Fig. 7A). To the mixture when only the target H1N1 is introduced, the as-synthesized Ag NCs indeed show a significant fluorescence enhancement at 580 nm (Fig. 7B). However, what needs to be emphasized is that its fluorescence intensity is weaker compared to that in Fig. 3B, which is attributed to the effect of Mg^{2+} in buffer. As shown in Fig. S13 (ESI†), the fluorescence intensity of the H1N1 probe/H1N1-Ag NCs in buffer with Mg^{2+} is weaker than that in buffer without Mg^{2+}. It is reported that Mg^{2+} has an effect that cannot be ignored on nucleic acid structures and functions [38–40]. Because DNA is a negatively charged biopolymer due to the existence of the phosphate groups, the cations mainly including Mg^{2+}, K^+, and Na^+ and water molecules are responsible for the structural stability and functions of DNA by the electrostatic interaction, and Mg^{2+} may promote the dimerization of structure. Hence, the secondary structural change of DNA template induced by Mg^{2+} affects the fluorescence performance of the as-synthesized Ag NCs. Meanwhile, to the mixture when only the target H5N1 is added, the as-synthesized Ag NCs generate a strong emission at 605 nm (Fig. 7C) instead of 625 nm in unitary system (curve c in Fig. S3B ESI†). The shift of maximum emission wavelength may be interpreted as the influence of the change of microenvironments on the synthesis of Ag NCs in multiplexed detection [35]. Furthermore, to the mixture when only the target HIV is added, a strong fluorescence signal is exhibited at 680 nm (Fig. 7D). More importantly, the strong fluorescence emissions at 580, 605, and 680 nm are observed (Fig. 7E) when three targets are introduced simultaneously to the mixture of three probes, indicating that the simultaneous detection of different targets has little influence on each other. In conclusion, the proposed molecular beacon succeeds in realizing simultaneous detection of multiple targets.

3.4. Detection of target DNA in fetal bovine serum

To explore the sensing performance of the proposed biosensor in complex biological medium, the recovery experiment is carried out in fetal bovine serum sample. Three different concentrations of targets are spiked with 1% fetal bovine serum sample and the obtained recoveries are listed in Table S4 (ESI†). These analytical results demonstrate that our sensor method has an applicable potential in real biological sample.

4. Conclusions

In conclusion, we develop a molecular beacon based on DNA-templated Ag NCs for the highly sensitive and selective detection of target gene. By embedding different recognition sequences, the molecular beacon can be conveniently used for versatile detection of different targets. Furthermore, by circumventing overlap of the emission spectra, the constructed probes present a great potential in simultaneous detection of the multiple target genes. In view of these advantages mentioned above, this design may be used for multiplexed analysis of the other biologically relevant molecules with easy operation and low cost in the future.

Acknowledgments

This work was supported by the National Natural Science Foundation of China (21171108), Shanxi Provincial Fund for Natural Sciences (201601D011026).

Appendix A. Supplementary material

Supplementary data associated with this article can be found in the online version at http://dx.doi.org/10.1016/j.talanta.2017.12.049.

References

[1] H.-Z. He, D.S.-H. Chan, C.-H. Leung, D.-L. Ma, A highly selective G-quadruplex-based luminescent switch-on probe for the detection of gene deletion, Chem. Commun. 48 (2012) 9462–9464.
[2] S.F. Lee, M.A. Osborne, Photodynamics of a single quantum dot: fluorescence activation, enhancement, intermittency, and decay, J. Am. Chem. Soc. 129 (2007) 8936–8937.
[3] Y. Xiao, Z.J. Wu, K.Y. Wong, Z.H. Liu, Hairpin DNA probes based on target induced in situ generation of luminescent silver nanoclusters, Chem. Commun. 50 (2014) 4849–4852.
[4] I. Dıez, R.H.A. Ras, Fluorescent silver nanoclusters, Nanoscale 3 (2011) 1963–1970.
[5] B. Adhikari, A. Banerjee, Facile synthesis of watersoluble fluorescent silver nanoclusters and HgII sensing, Chem. Mater. 22 (2010) 4364–4371.
[6] Y.T. Su, G.Y. Lan, W.Y. Chen, H.T. Chang, Detection of copper ions through recovery of the fluorescence of DNA-templated copper/silver nanoclusters in the presence of mercaptopropionic acid, Anal. Chem. 82 (2010) 8566–8572.
[7] J. Peng, J. Ling, X.Q. Zhang, H.P. Bai, L.Y. Zheng, Q.E. Cao, Z.T. Ding, Sensitive detection of mercury and copper ions by fluorescent DNA/Ag nanoclusters in guanine-rich DNA hybridization, Sens. Actuators A 137 (2015) 1250–1257.
[8] Y. Zhu, X.C. Hu, S. Shi, R.R. Gao, H.L. Huang, Y.Y. Zhu, X.Y. Lv, T.M. Yao, Ultrasensitive and universal fluorescent aptasensor for the detection of biomolecules (ATP, adenosine and thrombin) based on DNA/Ag nanoclusters fluorescence light-up system, Biosens. Bioelectron. 79 (2016) 205–212.
[9] Z.Z. Huang, F. Pu, Y.H. Lin, J.S. Ren, X.J. Qu, Modulating DNA-templated silver nanoclusters for fluorescence turn-on detection of thiol compounds, Chem. Commun. 47 (2011) 3487–3489.
[10] K.S. Park, S.S. Oh, H.T. Sohbc, H.G. Park, Target-controlled formation of silver nanoclusters in abasic site-incorporated duplex DNA for labelfree fluorescence detection of theophylline, Nanoscale 6 (2014) 9977–9982.
[11] J. Sharma, H.C. Yeh, H. Yoo, J.H. Werner, J.S. Martinez, Silver nanocluster aptamers: in situ generation of intrinsically fluorescent recognition ligands for protein detection, Chem. Commun. 47 (2011) 2294–2296.
[12] K. Zhang, K. Wang, X. Zhu, M.H. Xie, A new signal-on method for the detection of protein based on binding-induced strategy and photoinduced electron transfer between Ag nanoclusters and split G-quadruplex-hemin complexes, Anal. Chim. Acta 887 (2015) 224–229.
[13] W.H. Li, W. Li, Y.F. Hu, Y.L. Xia, Q.P. Shen, Z. Nie, Y. Huang, S.Z. Yao, A fluorometric assay for acetylcholinesterase activity and inhibitor detection based on DNA-templated copper/silver nanoclusters, Biosens. Bioelectron. 47 (2013) 345–349.
[14] Y.X. Qian, Y.D. Zhang, L. Lu, Y.N. Cai, A label-free DNA-templated silver nanocluster probe for fluorescence on–off detection of endonuclease activity and inhibition, Biosens. Bioelectron. 51 (2014) 408–412.
[15] W. Yang, J.N. Tian, L.J. Wang, S. Fu, H.Y. Huang, Y.C. Zhao, S.L. Zhao, A new label-free fluorescent sensor for human immunodeficiency virus detection based on exonuclease III-assisted quadratic recycling amplification and DNA-scaffolded silver nanoclusters, Analyst 141 (2016) 2998–3003.
[16] Y.D. Ye, L. Xia, D.D. Xu, X.J. Xing, D.W. Pang, H.W. Tang, DNA-stabilized silver nanoclusters and carbon nanoparticles oxide: a sensitive platform for label-free fluorescence turn-on detection of HIV-DNA sequences, Biosens. Bioelectron. 85 (2016) 837–843.
[17] Q. Cao, Y. Teng, X. Yang, J. Wang, E.K. Wang, A label-free fluorescent molecular beacon based on DNA-Ag nanoclusters for the construction of versatile biosensors, Biosens. Bioelectron. 74 (2015) 318–321.
[18] K. Wang, D.Q. Fan, Y.Q. Liu, S.J. Dong, Cascaded multiple amplification strategy for ultrasensitive detection of HIV/HCV virus DNA, Biosens. Bioelectron. 87 (2017) 116–121.
[19] L.B. Zhang, J.B. Zhu, Z.X. Zhou, S.J. Guo, J. Li, S.J. Dong, E.K. Wang, A new

approach to light up DNA/Ag nanocluster-based beacons for bioanalysis, Chem. Sci. 4 (2013) 4004–4010.
[20] Y. Tao, M.Q. Li, J.S. Ren, X.G. Qu, Metal nanoclusters: novel probes for diagnostic and therapeutic applications, Chem. Soc. Rev. 44 (2015) 8636–8663.
[21] P. Shah, A.L. Rorvig, S.B. Chaabane, P.W. Thulstrup, H.G. Kjaergaard, E. Fron, J. Hofkens, S.W. Yang, T. Vosch, Design aspects of bright red emissive silver nanoclusters/DNA probes for microRNA detection, ACS Nano 6 (2012) 8803–8814.
[22] C.M. Ritchie, K.R. Johnsen, J.R. Kiser, Y. Antoku, R.M. Dickson, J.T. Petty, Ag nanocluster formation using a cytosine oligonucleotide template, J. Phys. Chem. C 111 (2007) 175–181.
[23] J.T. Petty, J. Zheng, N.V. Hud, R.M. Dickson, DNA-templated Ag nanocluster formation, J. Am. Chem. Soc. 126 (2004) 5207–5212.
[24] B.Y. Han, E.K. Wang, DNA-templated fluorescent silver nanoclusters, Anal. Bioanal. Chem. 402 (2012) 129–138.
[25] C.I. Richards, S. Choi, J.C. Hsiang, Y. Antoku, T. Vosch, A. Bongiorno, Y.L. Tzeng, R.M. Dickson, Oligonucleotide-stabilized Ag nanocluster fluorophores, J. Am. Chem. Soc. 130 (2008) 5038–5039.
[26] B. Sengupta, C.M. Ritchie, J.G. Buckman, K.R. Johnsen, P.M. Goodwin, J.T. Petty, Base -directed formation of fluorescent silver clusters, J. Phys. Chem. C 112 (2008) 18776–18782.
[27] J. Sharma, R.C. Rocha, M.L. Phipps, H.-C. Yeh, K.A. Balatsky, D.M. Vu, A.P. Shreve, J.H. Werner, J.S. Martinez, A. DNA-templated, Fluorescent silver nanocluster with enhanced stability, Nanoscale 4 (2012) 4107–4110.
[28] L.Y. Feng, Z.Z. Huang, J.S. Ren, X.G. Qu, Toward site-specific, homogeneous and highly stable fluorescent silver nanoclusters fabrication on triplex DNA scaffolds, Nucleic Acids Res. 40 (2012) e122.
[29] B. Sengupta, K. Springer, J.G. Buckman, S.P. Story, O.H. Abe, Z.W. Hasan, Z.D. Prudowsky, S.E. Rudisill, N.N. Degtyareva, J.T. Petty, DNA templates for fluorescent silver clusters and i-motif folding, J. Phys. Chem. C 113 (2009) 19518–19524.
[30] L.B. Zhang, J.B. Zhu, S.J. Guo, T. Li, J. Li, E.K. Wang, Photoinduced electron transfer of DNA/Ag nanoclusters modulated by G-quadruplex/hemin complex for the construction of versatile biosensors, J. Am. Chem. Soc. 135 (2013) 2403–2406.
[31] S. Link, M.A. El-Sayed, Spectral properties and relaxation dynamics of surface plasmon electronic oscillations in gold and silver nanodots and nanorods, J. Phys. Chem. B 103 (1999) 8410–8426.
[32] S. Ehud, S. Olaf, A.-S. Marcelo, G. Guido, D.F. Rosa, V. Fabrice, D.F. Natalia, B. Uri, S. Carsten, Absorption properties of metal–semiconductor hybrid nanoparticles, ACS Nano 5 (2011) 4712–4719.
[33] K.L. Kelly, E. Coronado, L.L. Zhao, G.C. Schatz, The optical properties of metal nanopartic -les: the influence of size, shape, and dielectric environment, J. Phys. Chem. B 107 (2003) 668–677.
[34] W. Li, L. Liu, Y. Fu, Y.H. Sun, J.L. Zhang, R.X. Zhang, Effects of polymorphic DNA on the fluorescent properties of silver nanoclusters, Photochem. Photobiol. Sci. 12 (2013) 1864–1872.
[35] E.G. Gwinn, P. O'Neill, A.J. Guerrero, D. Bouwmeester, D.K. Fygenson, Sequence-dependent fluorescence of DNA-hosted silver nanoclusters, Adv. Mater. 20 (2008) 279–283.
[36] M. Vorlickova, I. Kejnovska, K. Bednarova, D. renciuk, J. Kypr, Circular dichroism spectros spectroscopy of DNA: from duplexes to quadruplexes, chirality 24 (2012) 691–698.
[37] J. Kypr, I. Kejnovska, D. Renciuk, M. Vorlıckova, Circular dichroism and conformational polymorphism of DNA, Nucleic Acids Res. 37 (2009) 1713–1725.
[38] F. Leonarski, L. D'Ascenzo, P. Auffinger, Mg^{2+} ions: do they bind to nucleobase nitrogens? Nucleic Acids Res. 45 (2017) 987–1004.
[39] S. Saxena, S. Joshi, J. Shankaraswamy, S. Tyagi, S. Kukreti, Magnesium and molecular crowding of the cosolutes stabilize the i-motif structure at physiological pH, Biopolymers 107 (2017) e23018.
[40] S. Paul, T. Ahmed, A. Samanta, Influence of divalent counterions on the dynamics in DNA as probed by using a minor-groove binder, ChemPhysChem 18 (2017) 1–8.